Intention-aware prediction for collaborative collision avoidance in manned-unmanned mixed maritime traffic

Ocean Engineering 356 (2026) 125131

Contents lists available at ScienceDirect

Ocean Engineering

journal homepage: www.elsevier.com/locate/oceaneng

Research paper

Intention-aware prediction for collaborative collision avoidance in manned-unmanned mixed maritime traffic ☆

Dhanika Mahipala [a,*], Hoang Anh Tran [b], Rana Saha [c], Tor Arne Johansen [b,*]

[a] Advanced Manoeuvring & Vessel Autonomy, Kongsberg Maritime AS, Norway
[b] Department of Engineering Cybernetics, Norwegian University of Science and Technology, Norway
[c] Chalmers School of Maritime Studies, Chalmers University of Technology, Sweden

ARTICLE INFO

Keywords:
Autonomous ship
Collision avoidance
Dynamic Bayesian network
Intention inference
Model predictive control

ABSTRACT

Communication between vessels is critical for successful collision avoidance. In conventional marine navigation, where all vessels have human crew on board, such a task is trivial. However, with the rise of interest in autonomous vessels, we could expect marine traffic scenarios where both manned and unmanned vessels co-exist for a long period of time until the entire maritime industry fully transitions to autonomous vessels. Implementing a collaborative collision avoidance algorithm in an unmanned vessel in such an environment could be challenging due to the lack of modern computational equipment on board a traditional manned vessel. In this paper, we present an approach that allows collaborative collision avoidance between manned and unmanned vessels. We extend an existing collaboration framework designed for unmanned vessels utilizing a Dynamic Bayesian Network (DBN) to model the response behavior of the manned vessel, enabling manned and unmanned vessel collaboration. A simulation study is used to verify the applicability of the proposed approach and to evaluate its performance.

1. Introduction

Effective communication is critical to ensure safe navigation of vessels, particularly if there is any risk of collision. Although the International Regulations for Preventing Collisions at Sea (COLREGs), 1972 specify a legal framework for collision avoidance, practical scenarios often require vessel-to-vessel direct communication (International Maritime Organization (IMO), 1972) to enhance safety, efficiency and flexibility. In complex scenarios, blindly following COLREGs without communication can lead to misinterpretations, delays, or unsafe maneuvers. Using VHF radio, Automatic Identification System (AIS) messages, and sound signals, vessels can confirm intentions and coordinate actions, leading to a more scalable, optimal, and proactive approach to collision avoidance.

To support the ongoing development on maritime automation, the International Maritime Organization (IMO) introduced four different levels of automation (LoA), where LoA 3 and LoA 4 cover remotely controlled unmanned vessel and fully autonomous vessel, respectively (International Maritime Organization (IMO), 2018). However, upon introduction of unmanned vessels, conventional vessels with automated processes and decision support (LoA 1) and remotely controlled manned vessel (LoA 2) will still be navigating on the same waterways. Therefore, traditional human-to-human communication during vessel operation is expected to also encounter 'machine-to-machine' (M-M) communication and 'human-to-machine' (H-M) communication in mixed traffic scenarios (Saha et al., 2023). In order to ensure safe and efficient navigation and collision avoidance, this communication should be standardized and machine compatible.

The M-M collaboration has been receiving significant interest from the research society. Several solutions have been proposed to address the problem of a collaborative collision avoidance system (CCAS) for autonomous ships (Chen et al., 2018; Ferranti et al., 2018; Akdağ et al., 2024b; Tran et al., 2025). The CCAS solutions can be categorized as indirect negotiation (Akdağ et al., 2024b; Chen et al., 2018) and direct negotiation (Ferranti et al., 2018; Tran et al., 2025). In indirect negotiation, ships only share their intended trajectories and do not directly request other ships to change course. This type of CCAS solution can also be directly applied to manned ships to become H-M collaboration

☆ The research leading to these results has received funding from the European Union's Horizon 2020 research and innovation program under the Marie Skłodowska-Curie grant agreement No 955.768 (MSCA-ETN AUTOBarge). This publication reflects only the authors' view, exempting the European Union from any liability. Project website: http://etn-autobarge.eu/.

* Corresponding authors.
E-mail addresses: dhanika.mahipala@km.kongsberg.com (D. Mahipala), hoang.a.tran@ntnu.no (H.A. Tran), rana.saha@chalmers.se (R. Saha), tor.arne.johansen@ntnu.no (T.A. Johansen).

https://doi.org/10.1016/j.oceaneng.2026.125131
Received 3 October 2025; Received in revised form 25 February 2026; Accepted 15 March 2026
Available online 28 March 2026

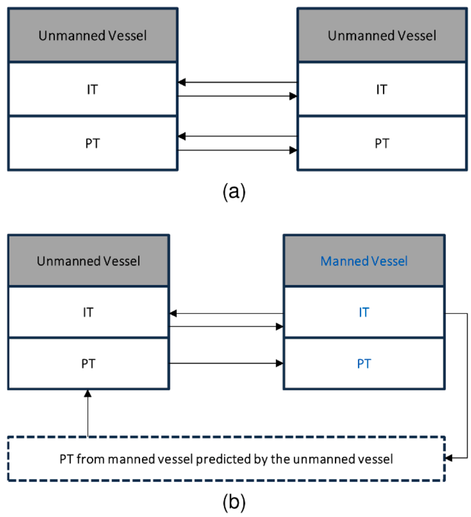

Fig. 1. (a) M-M communication in CCAS-Proto (b) Proposed H-M communication to fulfill CCAS-Proto.

by requiring the manned ships to share their intention (Akdağ et al., 2022; Akdağ et al., 2024a). In contrast, in direct negotiation, a ship can directly influence the decision of other neighboring ships. The main advantage of direct negotiation is that a ship can request others to change course if the situation requires it. For this reason, we believe that direct negotiation is the most promising direction for developing CCAS. Based on this, we have selected the method proposed in Tran et al. (2025) as the foundation for our work, and we aim to extend it to support the H-M collaboration. This specific CCAS is especially suitable because, unlike (Ferranti et al., 2018), it takes into account local traffic rules when making decisions.

The M-M CCAS algorithm introduced in Tran et al. (2025) includes a two-part protocol designed to facilitate data exchange between vessels. For clarity and brevity, we will refer to the algorithm as **MM-CCAS** and the communication protocol as **CCAS-Proto** throughout this paper. The CCAS-Proto consists of the following two components:

- Intended Trajectory (**IT**) - the planned path the ship aims to follow.
- Proposed Trajectory (**PT**) - suggested trajectory adjustment for the other ship to follow.

As illustrated in Fig. 1a, MM-CCAS assumes that both unmanned vessels will be capable of sharing IT and PT. However, in a H-M communication setting, which is the focus of this research, it is significantly more difficult for manned vessels to share PT with unmanned counterparts. Neither current regulation requires such digital collaboration, nor is the existing CCAS ready to address this. This raises the research question whether the H-M communication can be completed according to the same CCAS-Proto by predicting the PT from the manned vessel by the unmanned vessel itself as shown in Fig. 1b, granted the former has the capability to share its IT as required by the first step of the protocol.

AIS is a mandatory navigational tool for commercial vessel operation under the IMO's SOLAS regulations (Chapter V, Regulation 19). According to current law, an AIS is designed to share the navigation state of the vessel, that is, position, course, speed, heading, turn rate, and navigational status, almost in real time while moving (International Maritime Organization (IMO), 1972) (International Maritime Organization (IMO), 2015) (Navigation, 2016). In support of ongoing efforts for autonomous navigation within a secured cyberspace, the International Hydrographic Organization (IHO) proposed standardized digital data exchange under the S-100 framework (International Hydrographic Organization (IHO), 2020),(International Hydrographic Organization, 2025). It serves as a modern and versatile standard for creating and sharing digital products and services related to hydrography, maritime navigation, and geographic information systems (GIS).

S-421 is an S-100 compliant product specification developed to standardize the digital exchange of route plans between maritime navigation and radio communication systems. It provides a framework for the exchange of route information between vessels and shore authorities. Once implemented, the IT sharing part of the CCAS-Proto can expect to be fulfilled by a manned vessel. If the PT of the manned vessel can be predicted by the unmanned vessel, the CCAS-Proto can be completed as illustrated in Fig. 1b. Therefore, in this research, our aim is to propose a novel CCAS algorithm that enables CCAS in both H-M and M-M mixed traffic scenarios. We will refer to this algorithm as **HM-CCAS** throughout this paper.

The trajectory of a vessel in situations that involve a risk of collision is influenced by its inherent characteristics, such as size, speed, and type, as well as external factors, including COLREGs, the surrounding environment of the trajectory, and other situational conditions. These factors shape the underlying intentions of each individual vessel, guiding how it plans to maneuver in the potential collision scenario. For example, whether the vessel intends to comply with the COLREGs and, if so, what it considers to be an appropriate reaction time or safe passing distance can be characterized as underlying intentions.

Hence, to predict PT for the unmanned vessel, its underlying intentions should first be identified. If the manned vessel is assigned to provide PT, the underlying intentions of the unmanned vessel are inferred by human operators based on its behavior during the encounter. Therefore, when attempting to generate the PT by the unmanned vessel from the manned vessel's perspective, our hypothesis is that it is justifiable to use a probabilistic approximation of the intentions derived from available AIS data instead.

Recently, Rothmund et al. (2022), proposed a Dynamic Bayesian Network (DBN) (Dagum et al., 1992; Koller and Friedman, 2009) model that takes into account multiple underlying causes, allowing different interpretations of the situation by different vessels. Various authors have proposed several improvements and verification strategies. In article (Rothmund et al., 2023), the said intention model was validated using real-world encounters extracted from historical AIS data. The authors of Tengesdal et al. (2024) use the model in a collision avoidance algorithm and validate the result in a real-time experimental setting. In Mahipala et al. (2025), researchers propose changes to the model to be able to utilize information on planned routes and grounding hazards to improve its predictions.

The model proposed in Mahipala et al. (2025) can be used to infer probability distributions of the underlying intentions of the unmanned vessel. These distributions approximate how the manned vessel might perceive the intentions of the unmanned vessel. As demonstrated in Mahipala et al. (2025), the same DBN can also be used to evaluate whether a certain trajectory also aligns with a set of given intentions. Our hypothesis is that we can effectivly use this to propose a PT for the unmanned vessel. The contributions in this paper are as follows:

- A novel CCAS algorithm (HM-CCAS) that enables collision avoidance in H-M and M-M mixed traffic scenarios.
- Adaptation and repurposing of the intention model proposed in Mahipala et al. (2025) for the task of predicting PT in HM-CCAS. This includes the use of future trajectories from the CCAS, rather than using merely the current navigation states.
- Verification and validation of the proposed algorithm through a comprehensive simulation study involving one manned and one unmanned ship.

2. Collaborative collision avoidance framework

The H-M CCAS framework is based on the M-M framework for collaboration between unmanned ships introduced in Tran et al. (2025). This section first briefly presents the M-M framework concept, where more details can be found in Tran et al. (2025). Next, we introduce a method to incorporate manned ships into the M-M CCAS framework.

2.1. M-M collaborative collision avoidance framework

Let us consider the set $\mathcal{M}$ of M unmanned ships. Each ship $i \in \mathcal{M}$ is assumed to perceive the surrounding environment independently. We assume each ship uses a local coordinate frame $\{\varpi_i\}$ to represent its navigation state and uses an inertial coordinate frame $\{n\}$ to share information with others. The navigation state of ship i perceived by itself at time step k from the current time $t = t_0$ is denoted as follows:

$$p_{i,i}(t_0+k) = \begin{bmatrix} x_{i,i}(t_0+k) \\ y_{i,i}(t_0+k) \\ \chi_{i,i}(t_0+k) \end{bmatrix},$$

where $x_{i,i}, y_{i,i}$ are position information and $\chi_{i,i}$ is the course angle information. Similarly, the navigation state of ship j perceived by ship i at time step k is as follows:

$$p_{j,i}(t_0+k) = \begin{bmatrix} x_{j,i}(t_0+k) \\ y_{j,i}(t_0+k) \\ \chi_{j,i}(t_0+k) \end{bmatrix}.$$

Furthermore, the IT of ship i over a control horizon of N time steps is defined as:

$$\tilde{p}_{i,i}(t_0+k) = [p_{i,i}^\top(t_0), p_{i,i}^\top(t_0+1), ..., p_{i,i}^\top(t_0+N)]^\top,$$

and the PT from ship i to ship j in the same period is defined as:

$$\tilde{p}_{j,i}(t_0+k) = [p_{j,i}^\top(t_0), p_{j,i}^\top(t_0+1), ..., p_{j,i}^\top(t_0+N)]^\top.$$

In the M-M collaboration framework, ships exchange their IT, i.e., $p_{i,i}$, and their PTs, i.e., $p_{j,i}\ \forall j \in \mathcal{M} \setminus \{i\}$. The M-M collaboration framework aims to reach a consensus solution between ships. If we define the consensus solution as the future navigation state of all ships in $\mathcal{M}$ with respect to the inertial coordinate frame $\{n\}$ as ξ. Then, the consensus condition can be expressed as:

$$\begin{aligned} \tilde{p}_i &= \mathrm{I}_{3MN} \otimes R_i(\xi - \mathbf{1}_{3MN} \otimes c_i) = \tilde{R}_i(\xi - \tilde{c}_i), \\ \tilde{p}_i &= \left[\tilde{p}_{i,1}^\top, \tilde{p}_{i,2}^\top, \dots, \tilde{p}_{i,M}^\top\right]^\top, \\ \tilde{R}_i &= \mathbf{diag}(R_1, \dots, R_M), \\ \tilde{c}_i &= [c_1^\top, \dots, c_M^\top]^\top, \end{aligned} \tag{1}$$

where $\tilde{p}_i$ is the vector that contains the IT and PTs from ship i; R_i and c_i are, respectively, the rotation matrix from $\{n\}$ to $\{\varpi_i\}$ and the origin displacement between two coordinates. Here, $\otimes$ denotes the Kronecker product.

The M-M collaboration framework is made up of three components as follows.

2.1.1. Trajectory prediction of ships

To predict the future risk of collision, it is important to predict the future position of both the ownship and other target ships. Each ship i uses two types of kinematic models: the kinematic model of the ownship and the kinematic model of neighboring ships. The kinematic model of the ownship is written as

$$p_{i,i}(k+1) = f_{i,i}(p_{i,i}(k), u_{i,i}(k)), \tag{2}$$

while the kinematic model of a neighboring ship j is written as

$$p_{j,i}(k+1) = f_{j,i}(p_{j,i}(k), u_{j,i}(k)). \tag{3}$$

In (2) and (3), $u_{i,i}(k), u_{j,i}(k) \in \mathbb{R}^2$ are the input control signals consisting of the course and speed references. The details of the kinematic models are out of the scope of this paper, but they are well known and can be found in, for example, Tran et al. (2025). Here, we assume that the kinematic models of the neighboring ships are known beforehand through exchanging information between ships.

2.1.2. Collision risk evaluation

The risk of collision between ship i and j predicted by ship i is expressed as follows:

$$\begin{aligned} R_{ij}(t_0+k) &= \frac{K_{ca}}{\sqrt{1+K_d k}} D_x(t_0+k) D_y(t_0+k), \\ D_x(t_0+k) &= exp\left[-\frac{\left(x_{i,i}(t_0+k) - x_{j,i}(t_0+k)\right)^2}{\alpha_{xj}}\right], \\ D_y(t_0+k) &= exp\left[-\frac{\left(y_{i,i}(t_0+k) - y_{j,i}(t_0+k)\right)^2}{\alpha_{yj}}\right], \end{aligned} \tag{4}$$

where K_{ca}, K_d are tuning parameters, and α_{xj}, α_{yj} are the safety parameters depending on the size and shape of ship j. More details of the risk function can be found in Tran et al. (2024).

2.1.3. Decision making algorithm

This is the core part of the M-M CCAS framework. Based on the risk evaluation, a distributed model predictive control (DMPC) algorithm is used to decide the action to avoid collisions. According to Tran et al. (2025), the DMPC problem of ship i can be formulated as follows:

$$\min_{\tilde{p}_i, \tilde{u}_i} \quad \mathcal{J}_i(\tilde{p}_i, \tilde{u}_i) \tag{5a}$$

$$\text{s.t.:} \quad p_{i,i}(t_0+k+1) = f_{i,i}(p_{i,i}(t_0+k), u_{i,i}(t_0+k)), \tag{5b}$$

$$p_{j,i}(t_0+k+1) = f_{j,i}(p_{j,i}(t_0+k), u_{j,i}(t_0+k)), \tag{5c}$$

$$u_{i,i}(t_0+k) \in \mathcal{U}_i, \tag{5d}$$

$$u_{j,i}(t_0+k) \in \mathcal{U}_{j,i} \tag{5e}$$

$$\tilde{p}_i = \tilde{R}_i(\xi - \tilde{c}_i). \tag{5f}$$

Here $\tilde{u}_{i,i} = [u_{i,i}^\top(t_0), u_{i,i}^\top(t_0+1), ..., u_{i,i}^\top(t_0+N-1)]^\top$ is the control vector for all ships, and $\mathcal{U}_i$ and $\mathcal{U}_{j,i}$ are the boundary set of $u_{i,i}$ and $u_{j,i}$ respectively. Additionally, $\tilde{u}_i = \left[\tilde{u}_{i,1}^\top, \tilde{u}_{i,2}^\top, \dots, \tilde{u}_{i,M}^\top\right]^\top$ is the vector contains all $\tilde{u}_{i,j}, j \in \mathcal{M}$.

The cost function $\mathcal{J}_i(\tilde{p}_i, \tilde{u}_i)$ is defined following (Tran et al., 2025) as:

$$\mathcal{J}_i(\tilde{p}_i, \tilde{u}_i) = \mathcal{J}_i^{ca}(\tilde{p}_i) + \mathcal{J}_i^{e}(\tilde{u}_i) + \mathcal{J}_i^{b}(\tilde{u}_i), \tag{6}$$

where $\mathcal{J}_i^{ca}(\tilde{p}_i) = \sum_{k=1}^{N+1} \sum_{j \in \mathcal{M} \setminus \{i\}} R_{ij}(t_0+k)$ is the sum of risk functions caused by all other neighboring ships. Reducing $\mathcal{J}_i^{ca}(\tilde{p}_i)$ allows ship i to reduce the collision risk and increase the safety navigation. $\mathcal{J}_i^{e}(\tilde{u}_i)$ and $\mathcal{J}_i^{b}(\tilde{u}_i)$ are the cost of control actions and behavior cost, respectively. Reducing $\mathcal{J}_i^{e}(\tilde{u}_i)$ and $\mathcal{J}_i^{b}(\tilde{u}_i)$ helps ship i to decrease the deviation from the nominal path and comply with traffic regulations (see Tran et al. (2024) for more details).

Remark 1. In (6), N is the prediction horizon of the DMPC problem. N should be chosen carefully, as a small value of N makes ships less aware of incoming risk. On the other hand, a large value of N could increase computational complexity. Furthermore, predictions that are too far in the future tend to be inaccurate and make a minor contribution to risk evaluation.

Problem (5) is solved using the Asynchronous CCAS algorithm, also called Algorithm 1. In Algorithm 1, the set $\mathbf{G}_i$ is the feasible region for the states and inputs of ship i that satisfies constraints (5b)–(5f), and z_i is the vector of Lagrange multipliers. $\mathcal{L}_i(\tilde{p}_i, \tilde{u}_i)$ is the augmented Lagrangian of problem (5) and is defined as:

$$\mathcal{L}_i(\tilde{p}_i, \tilde{u}_i) = \mathcal{J}_i(\tilde{p}_i, \tilde{u}_i) + \left\langle z_i^{s+1/2}, \tilde{R}_i^{-1}\tilde{p}_i + \tilde{c}_i - \xi^{s+1} \right\rangle + \frac{\beta}{2}\left|\left|\tilde{R}_i^{-1}\tilde{p}_i + \tilde{c}_i - \xi^{s+1}\right|\right|^2.$$

where s is the iteration index. Moreover, $\hat{\xi}_i$ is the local version of ξ send from ship i, and is obtained by convert $\tilde{p}_i$ to inertial coordinate frame $\{n\}$.

Algorithm 1: Async-CCAS.

Input: $\lambda \in (0,2)$, $\beta > 0$, initiate $\tilde{p}_i$ using constant velocity model.

for $s = 1, \ldots, s_{\max}$ **do**
  for all $i \in \mathcal{M}$ each ship computes in parallel **do**
    Receive $\hat{\xi}_j^s$ from neighboring ships, $j \in \mathcal{M}\backslash\{i\}$
    if $\hat{\xi}_j^s$ is unavailable **then**
      $\hat{\xi}_j^s = \hat{\xi}_j^{s-1}$
    end if
    $\xi_j^{s+1} = \frac{1}{M}\sum_{j=1}^{M}\hat{\xi}_j^s$
    $z_i^{s+1/2} = z_i^s - \beta(1-\lambda)\left(\tilde{R}_i^{-1}\tilde{p}_i^s + \tilde{c}_i - \xi_j^{s+1}\right)$
    $\begin{bmatrix}\tilde{u}_i^{s+1}\\ \tilde{p}_i^{s+1}\end{bmatrix} = \mathrm{argmin}_{[\tilde{u}_i^\top, \tilde{p}_i^\top]^\top \in \mathbf{G}_i}\left\{\mathcal{L}_i(\tilde{p}_i, \tilde{u}_i)\right\}$
    $z_i^{s+1} = z_i^{s+1/2} + \beta\left(\tilde{R}_i^{-1}\tilde{p}_i^{s+1} + \tilde{c}_i - \xi_j^{s+1}\right)$
    $\hat{\xi}_j^{s+1} = \tilde{R}_i^{-1}\tilde{p}_i^{s+1} + \tilde{c}_i + \frac{1}{\beta}z_i^{s+1}$
    Transmit data $\hat{\xi}_i^s$ to all ship $j \in \mathcal{M}\backslash\{i\}$.
  end for
end for

2.2. H-M collaborative collision avoidance framework

Considering a mixed traffic scenario with both manned and unmanned ships participating. For a manned ship participating in the M-M CCAS in Section 2.1, two requirements need to be achieved. The first requirement is that the solution provided by the manned ship is compatible to that provided by the unmanned ships. The second requirement is providing the PT information, i.e., $p_{j,i}$, of the manned ship.

Considering the first requirement, there may be no systematic way to guarantee this due to the unstructured nature of human decisions. However, it is reasonable to assume that the manned ship wants to avoid collision by following the traffic regulations with minimum deviation from the current path. Using this assumption and the cost function defined in (6), the solution of the manned ship will contribute to reducing the cost function and progress toward the optimal solution.

While a human pilot with support from a digital control system can send out their intended trajectory, it is unrealistic to require a manned ship to provide its PT for the unmanned ship in the same format as communicated and used by unmanned ships in a limited negotiation time. An approach to overcome this obstacle is to predict the PT from the manned ship, where the hypothesis is that the said DBN intention model can provide a prediction of the unmanned ship's behavior that can be used for this purpose. The prediction needs to be as accurate as possible because, in direct negotiation, the PT can directly affect a ship's decision. However, as the PT only partly contributes to the decision of the unmanned ships, it is allowed that the PT prediction is somewhat inaccurate. For example, if the manned ship wants an unmanned ship to reduce speed by 50%, it may be acceptable if the PT prediction predicts a reduction ranging from 40% to 60%. The difference in the timestamp between ships could be an issue for information sharing and predicting PT. However, it can be addressed by shifting one (or a few) time steps of the trajectory, depending on how large the difference in timestamp is. The details of the PT prediction method are presented in the following section.

3. Prediction of trajectory proposal (PT)

This section aims to describe how the DBN proposed in Mahipala et al. (2025) is repurposed to predict the required PT from the manned vessel for the unmanned vessel. There are three main stages in this method. In the first stage, the intentions of the unmanned vessel are predicted from the point of view of the manned vessel. In the second stage, several candidate trajectories are generated that cover the navigable area, account for both port and starboard maneuvers, and consider vessel dynamics. In the third and final stage, each candidate trajectory is evaluated to obtain the maximum probability of compliance with the predicted intentions.

3.1. Dynamic Bayesian network

The DBN used in this paper is a simplified version of the model presented in Mahipala et al. (2025). In this model, the waypoint consideration functionality has been removed and the grounding hazard consideration has been restricted to only account for hazards on either side of the vessel. These modifications were made to simplify the model, as they do not directly impact the focus of this research. The model identifies two roles: *reference vessel* and *obstacle vessel* (Mahipala et al., 2025), where the DBN infers the intentions of the reference vessel in encounters with the obstacle vessel. In the context of the present research, the *reference vessel* refers to the unmanned vessel, while the *obstacle vessel* refers to the manned vessel. The simplified DBN structure for a single ship encounter is depicted in Fig. 2.

The DBN includes three types of nodes within the context of the proposed network: intention nodes (denoted by I), measurement nodes (denoted by $\mathcal{M}$) and model nodes. Intentions are assumed to remain constant throughout an encounter and are thus represented as time-independent nodes, while both measurement and model variables are time-dependent. Intention and measurement nodes can be either binary ("true" or "false"), or real-valued, with multiple states representing value ranges specific to the variable's context. In contrast, the model nodes are composed exclusively of binary nodes. The definitions of these nodes are summarized in Tables 1 and 2.

For brevity, only the modified model nodes are explained in this paper and they are presented in the Appendix A. The readers are encouraged to refer to Mahipala et al. (2025) for the rest of the node definitions and more information on each node.

3.2. Algorithm

The process of using the proposed DBN for the prediction of PT in real time can be divided into several steps. First, the DBN should be initialized by clearing all evidence and setting the number of time slices to one. Next, within every execution cycle, the following steps are executed:

- **Step 1:** Extract navigation state information of the vessels from AIS data, sensors and their ITs.
- **Step 2:** Calculate the probability distributions of the intention variables in the DBN.
  - **Step 2-A:** Calculate the state estimates for the measurement nodes using the information extracted in **Step 1**.
  - **Step 2-B:** Set evidence for the measurement nodes using the estimates of **Step 2-A**.
  - **Step 2-C:** Set the evidence for the node variable C to *true* (see (A.5) in the Appendix A).
  - **Step 2-D:** Update the network beliefs and find the probability distributions for the intention nodes.
- **Step 3:** Add a temporary time slice to the DBN.
- **Step 4:** Generate candidate trajectories for the *reference vessel*, i.e. the unmanned vessel. These are potential candidates for PT from the manned vessel for the unmanned vessel in HM-CCAS. See Section 3.4 for more information.
- **Step 5:** Evaluate each candidate trajectory in accordance with the intentions predicted in **Step 2**.
  - **Step 5-A:** Calculate the states of the measurement nodes and set evidence for the measurement nodes in the temporary time slice added in **Step 3**.
  - **Step 5-B:** Use the probability distributions of the intention nodes found in **Step 2** to establish virtual evidence of the intention nodes.

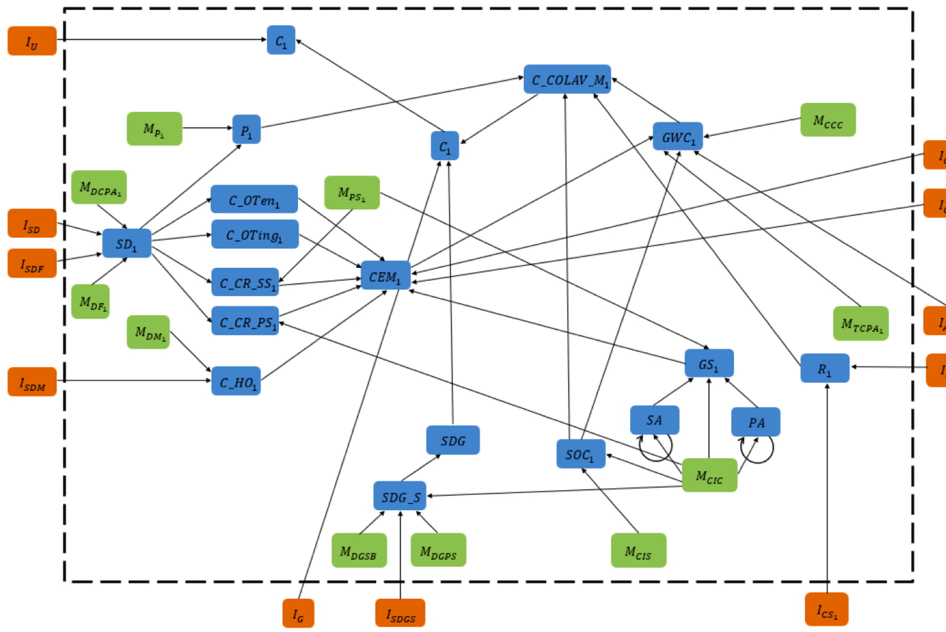

Fig. 2. Graphical representation of the topography of the proposed DBN for a single ship encounter. Subscript 1 indicates that this model considers the relation between the reference ship and the ship with index 1. All nodes within the box are time-dependent and are replicated at each time step. Circular arrows represent connections between consecutive time steps.

Table 1
Intention nodes.

Symbol	Description	States
I_{AT}	What time until CPA the reference ship considers ample time.	Real valued
I_{CC}	Whether the reference ship intends to be COLREGS-compliant when performing evasive maneuvers.	Binary
I_{GS}	Whether the reference ship acts according to good seamanship.	Binary
I_{P_i}	Whether the reference ship acts as if it has a lower or higher priority towards ship i.	"higher"/ "similar"/ "lower"
I_{CS_i}	What COLREGS situation the reference ship thinks it has towards ship i.	"OT_ing"/ "OT_en"/ "HO"/ "CR_PS"/ "CR_SS"
I_G	Whether the reference ship intends to sail towards a grounding hazard.	Binary
I_{SDGS}	What the reference ship considers a safe distance from either sides of the vessel to ground.	Real valued
I_{SD}	What the reference ship considers a safe distance at CPA.	Real valued
I_{SDF}	How far in front of a ship the reference ship considers a crossing as safe.	Real valued
I_{SDM}	What the reference ship considers a safe distance at CPA to the current midpoint.	Real valued
I_U	Whether the reference ship acts in an unmodeled way.	Binary

Table 2
Measurement nodes.

Symbol	Description	States
$\mathcal{M}_{DCPA_i}$	Distance between reference ship and ship i at CPA.	Real valued
$\mathcal{M}_{DF_i}$	How far the reference ship crosses in front on ship i. This value is set to ∞ if the ship does not cross in front of ship i.	Real valued
$\mathcal{M}_{DM_i}$	Distance at CPA to the current midpoint between the reference ship and ship i.	Real valued
$\mathcal{M}_{P_i}$	Whether reference ship has passed ship i.	Binary
$\mathcal{M}_{PS_i}$	Whether the reference ship will pass with ship i on its port or starboard side.	"starboard"/ "port"
$\mathcal{M}_{MPS_i}$	Whether the reference ship will pass the current midpoint between itself and ship i on its port or starboard side.	"starboard"/ "port"
$\mathcal{M}_{TCPA_i}$	Time until CPA between reference ships and ship i.	Real valued
$\mathcal{M}_{CIC}$	The change in course of the reference ship since the initial course at the start of the situation.	"starboard"/ "port"/ "straight"
$\mathcal{M}_{CIS}$	The change in speed of the reference ship since the initial speed at the start of the situation.	"higher"/ "lower"/ "none"
$\mathcal{M}_{CCC}$	Whether the reference ship is currently changing course.	Binary
$\mathcal{M}_{CS_i}$	Current COLREGS situation reference ship has towards ship i.	"OT_ing"/ "OT_en"/ "HO"/ "CR_PS"/ "CR_SS".
$\mathcal{M}_{DGSB}$	Current distance to the closest point of the ground hazard on the starboard side of the vessel.	Real valued
$\mathcal{M}_{DGPS}$	Current distance to the closest point of the ground hazard on the port side of the vessel.	Real valued

Step 5-C: Update the network beliefs and find the probability of the state of *true* at the node C. This is the probability of compatibility between that specific candidate trajectory and the intentions. Note that multiple trajectories can be compatible with intentions to varying degrees.

Step 6: Normalize and select the trajectory with the highest probability, that is, the "winning" trajectory. This trajectory is then used as the PT from the manned vessel in HM-CCAS.

Step 7: Delete the temporary time slice added to the network in **Step 3**.

Step 8: Add a new time slice.

In **Step 1**, the navigation state of the manned vessel is extracted along with the IT, that is, the position of East and North in Cartesian local coordinates, the course over the ground (COG) and the speed over the ground (SOG). The state of the unmanned vessel is also extracted from its sensors. **Step 2** describes how the intentions of the unmanned vessels are predicted from the point of view of a manned vessel.

In **Step 3**, a temporary time slice is added to the DBN to evaluate the compliance of each candidate trajectory with the predicted intentions. In **Step 4**, candidate trajectories were generated as explained in Section 3.4. Once each candidate trajectory is evaluated, the probability value of each candidate was subjected to a hard threshold of 0.5, zeroing out all values less than the threshold to exclude low-confidence trajectories. Finally, these values were normalized to obtain the confidence in each trajectory as a percentage value. Thresholding prevents values below the threshold from being artificially inflated during normalization. As mentioned in **Step 6**, the candidate with the highest percentage value is considered the "winning" trajectory and is used as the PT of the manned vessel for the unmanned vessel and is used in HM-CCAS. When there are multiple candidates with the highest percentage value, the trajectory farthest away from the manned vessel is considered the "winning" trajectory to maximize the safety margin due to the selection of trajectory from a discrete set.

Finally, after deleting the previously added temporary time slice in **Step 7**, it is evaluated whether a new time slice needs to be added to the DBN to predict intentions in the next step at **Step 8**. In an ideal scenario, a new time slice should be added at each time step to prevent data loss and improve prediction accuracy. However, the computation time of the DBN predictions increases exponentially with each added time slice. Hence, as proposed in Tengesdal et al. (2024), a condition can be added to aid with the decision. For example, a time slice can be added only when the previous time slice was created more than $\Delta_{ts,max}$ ago, or if the previous time slice was added no less than $\Delta_{ts,min}$ ago and any ship in the encounter has changed its course angle or speed by more than some threshold.

3.3. Changes to the measurement node calculations

Unlike (Mahipala et al., 2025), the trajectory of the *obstacle vessel* is considered known at every time step (IT of the manned vessel). Hence, the calculation of the state of each measurement node should be performed taking the entire trajectory into account. In this section, we aim to explain the node state calculations that require changes to facilitate this. First, we propose an algorithm that can be utilized to find the CPA of two trajectories.

In Algorithm 2, the corresponding states of the two trajectories are considered to calculate the distance at CPA, the time until CPA and the relative bearing at CPA denoted by $dcpa$, $tcpa$ and $Rcpa$, respectively. When the input to the binary variable in_fov is $True$, only the instances where the *obstacle vessel* is within the ± 12.5 range from the *reference vessel*'s course angle are considered. When predicting intentions in **Step 2**, $obstship\_traj$ refers to the IT of the manned vessel, i.e., *obstacle vessel* and $refship\_traj$ refers to the straight-line trajectory (assuming constant speed and course angle) of the unmanned vessel, i.e., *reference vessel*. The straight-line trajectory was used instead of the unmanned vessel IT since IT is the output of HM-CCAS. Using IT directly for the prediction of PT using DBN creates an internal loop within the algorithm that prevents the flow of new navigational information to the algorithm. When evaluating the compliance of the candidate trajectory in **Step 5**, $obstship\_traj$ refers to the same while $refship\_traj$ refers to the candidate trajectory in consideration. The input Δt refers to the sample time of the trajectories. The changes in the way the measurement nodes are calculated using Algorithm 2 are summarized in Table 3.

In Fig. 3, it is shown how the proposed algorithm uses the DBN to complete CCAS-Proto as indicated in Fig. 1b. As mentioned in Section 1, it is assumed that both vessls are capable of sharing IT. The unmanned vessel is able to share the PT, but the manned vessel cannot. Therefore, the IT of the manned vessel is used in **Step 2** and **Step 5** (see Section 3.2) as mentioned above to predict the PT of the manned vessel using the DBN.

Algorithm 2: *findCPA()* Find the closest point of approach (CPA).

Data: $refship\_traj, obstship\_traj, \Delta t, in\_fov$
Result: $tcpa, dcpa, Rcpa$
$dcpa \leftarrow \infty$;
$tcpa \leftarrow \infty$;
$Rcpa \leftarrow \infty$;
$t \leftarrow 0$;
foreach $refship\_state$ *and* $obstship\_state$ *in* $refship\_traj$ *and* $obstship\_traj$ **do**
  $t \leftarrow t + \Delta t$;
  $d \leftarrow$ current Euclidean distance between reference ship and obstacle ship;
  $R \leftarrow$ current relative bearing between reference ship and obstacle ship;
  if *not* in_fov *or* $abs(R) \leq 12.5°$ **then**
    if $d < dcpa$ **then**
      $dcpa \leftarrow d$;
      $tcpa \leftarrow t$;
      $Rcpa \leftarrow R$;
    end
  end
end

Table 3
Node-specific adaptations in the application of Algorithm 2.

Node	Input changes	Used output	Usage remarks
$\mathcal{M}_{DCPA_i}$	$in\_fov = False$	$dcpa$	–
$\mathcal{M}_{DF_i}$	$in\_fov = True$	$dcpa$	–
$\mathcal{M}_{P_i}$	$in\_fov = False$	$tcpa$	if $tcpa \leq 0$, then $\mathcal{M}_{P_i} = true$
$\mathcal{M}_{PS_i}$	$in\_fov = False$	$Rcpa$	if $Rcpa > 0$, then $\mathcal{M}_{PS_i} = port$

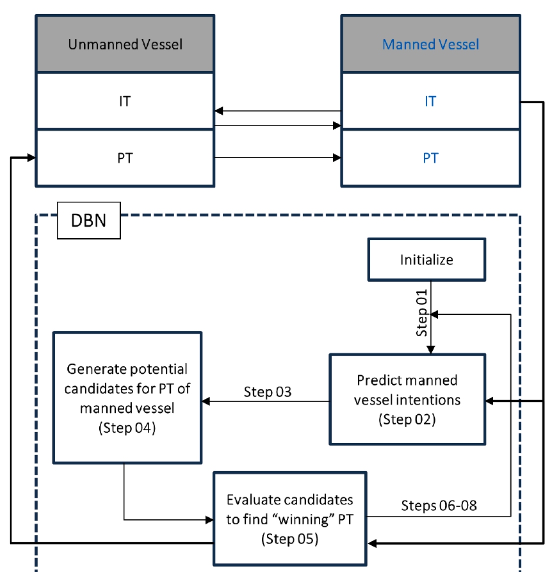

Fig. 3. How the proposed DBN complete CCAS-Proto by predicting the PT of the manned vessel.

3.4. Candidate trajectory generation

The way the candidate trajectory is generated is crucial for an acceptable PT. Here, we opt for generating multiple candidate trajectories for the reference (unmanned) vessel that take into account both starboard and port maneuvers, vessel dynamics, and the width of the navigable area of the waterway as illustrated in Fig. 4, where the reference

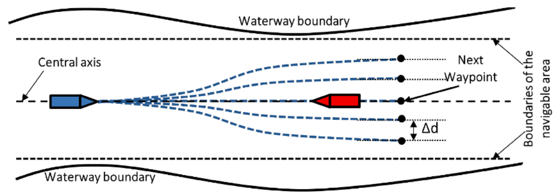

Fig. 4. Potential candidate trajectories, where the blue vessel is the unmanned (reference) vessel and the red vessel is the manned (obstacle) vessel.

(unmanned) vessel approaches the obstacle (manned) vessel from opposite sides of a waterway. The boundaries of the navigable area are determined in such a way that the next waypoint of the blue vessel falls on the central axis of the navigable area. The next waypoint of the unmanned vessel is then offset such that the width of the navigable area is divided into multiple zones, each of width Δd. The value of Δd can be determined depending on the expected distance between the vessels. These offsets, used to define the zone points, are alternate waypoints to avoid collisions with the manned vessel. From the current position of the unmanned vessel to each zone point, a trajectory (indicated by dashed blue lines) is generated using a Line-of-Sight (LOS) guidance controller and a simple ship model that reflect the unmanned vessel dynamics. Additionally, a separate set of trajectories can be generated assuming speed changes as well.

4. Results

The DBN model was developed using GeNie software (BayesFusion, 2021a), a graphical user interface to build and simulate Bayesian networks. Then it was integrated into a ship simulator via the Python wrapper of the SMILE Engine (BayesFusion, 2021b). The simulator was built using Python and was executed on a workstation equipped with an Intel Core i7-10750H CPU, 32 GB of RAM, and an NVIDIA RTX 2070 SUPER Mobile GPU.

To test the algorithm, a simulation setup is required that involves a minimum of two vessels, with at least one of them being a manned vessel. In the interest of brevity, we have chosen to include vessel encounters that involve only two vessels at a time. To evaluate the robustness of the algorithm, we considered different scenarios corresponding to different types of manned ship behavior: cooperative, non-cooperative, and traffic rules violation. The HM-CCAS algorithm is run at 20 second intervals and subfigures (a)–(g) in Figs. 5 to 8 show the position of the vessel at each time interval. In all four cases, the manned vessel ignores the PT of the unmanned vessel and chooses its own path attributed to typical human behavior. Hence, the PT of the unmanned vessel is not indicated in the figures.

The unmanned vessel evaluates seven candidate trajectories, namely p, q, r, s, t, u, and v, which can be considered the potential PT of the manned vessel using the proposed DBN. The candidate with the highest probability is used by the unmanned vessel as the PT of the manned vessel to complete the CCAS-Proto in HM-CCAS. For ease of comprehension, normalized trajectory probabilities are depicted as percentages in Figs. 5 to 8. The candidate trajectories are evaluated based on the IT of the manned vessel and therefore indicated on the figures. The IT of the unmanned vessel is also indicated as it is the output of the HM-CCAS which is followed by its control algorithm as reference to navigate the collision avoidance maneuver.

The subsequent chapters dive into how the DBN evaluates each trajectory to find the trajectory with the highest probability and how the HM-CCAS utilizes it to successfully avoid collision with the manned vessel. In addition, for comparison, each scenario is observed in which the unmanned vessel uses a straight-line trajectory generated using a Constant Velocity Model (CVM) as PT of the manned vessel.

Table 4
The likely intentions of the unmanned vessel, as perceived from the perspective of the manned vessel at $t = 40, 60, 100, 160s$ in Case Study 01.

Node ID	State			
	t = 40	t = 60	t = 100	t = 160
I_{SD}	State3	State3	State3	State3
I_{SDF}	State3	State3	State3	State3
I_{AT}	State4	State4	State4	State4
I_{CC}	true	true	true	true
I_{CS_1}	CR_PS	CR_PS	CR_PS	CR_PS
I_{GS}	true	true	true	true
I_{P_1}	similar	lower	lower	lower
I_{SDM}	State4	State4	State4	State4
I_U	false	false	false	false
I_G	false	false	false	false
I_{SDGS}	State3	State3	State3	State3

4.1. Case study 01

We consider a crossing situation involving a manned and an unmanned vessel. In this case study (see Fig. 5), we observe a normal crossing traffic situation with both ships cooperating to adhere to COLREGS. Consequently, the manned vessel turns to starboard to avoid collision while the unmanned vessel is expected to stand-on.

According to the DBN, it can be expected that the intentions of the unmanned vessel could be observed as shown in Table 4 at $t = 40, 60, 100, 160s$ instances.

The states of the modal variables in the DBN for each candidate trajectory at $t = 40s$ are shown in Table 5.

The DBN predicts that the unmanned vessel recognizes the COLREGS situation as a collision scenario from a port-side crossing incident ($I_{CS_1} = CR\_PS$). Since $I_{CS_1} = CR\_PS$ and the level of priority intended for the manned vessel (I_{P_1}) is predicted to be $similar$, the role of the unmanned vessel toward the manned vessel is evaluated as stand-on ($R_1 = SO$). As none of the candidates hasn't passed safely ($P_1 = false$) yet, for it to be a correct collision avoidance maneuver ($C\_COLAV\_M_1 = true$), it should be a stand-on correct maneuver ($SOC_1 = true$) and only the candidate s adheres to this requirement. Finally, since the unmanned vessel is not predicted to show unmodeled behavior ($I_U = false$), the aforementioned trajectory is evaluated as the only candidate trajectory in compliance with the predicted intentions ($C = true$).

At $t = 60s$, the states of the modal variables in the DBN for each candidate trajectory are shown in Table 6.

Since the course deviation of the manned vessel to give-way to the unmanned vessel is small, the level of priority intended for the manned vessel (I_{P_1}) is now predicted to be $lower$ assigning a give-way role to the unmanned vessel ($R_1 = GW$). Hence, for a candidate trajectory to be a correct collision avoidance maneuver ($C\_COLAV\_M_1 = true$), it should be a correct give-way ($GWC_1 = true$). The DBN predicts that the unmanned vessel intends to show good seamanship ($I_{GS} = true$). The DBN also predicts that the unmanned vessel intends to comply with COLREGS ($I_{CC} = true$) and that the intended COLREGS situation is a port-side crossing ($I_{CS_1} = CR\_PS$). Since candidate trajectories t, u, and v show correct port-side crossing compliant maneuvers ($C\_CR\_PS_1 = true$) and adhere to good seamanship conditions ($GS_1 = true$), they are evaluated as correct evasive maneuvers ($CEM_1 = true$) and in turn, correct give-way maneuvers ($GWC_1 = true$).

From $t = 60s$ to $t = 80s$ the conditions remain the same, and thus the t, u, v trajectories remain compliant with intentions. At $t = 100s$, the states of the modal variables in the DBN for each candidate trajectory are shown in Table 7.

Intentions have not changed since $t = 60s$. However, only candidates u and v satisfy good seamanship ($GS_1 = true$) and correct port side crossing requirements ($C\_CR\_PS_1 = true$) due to the advancements of the

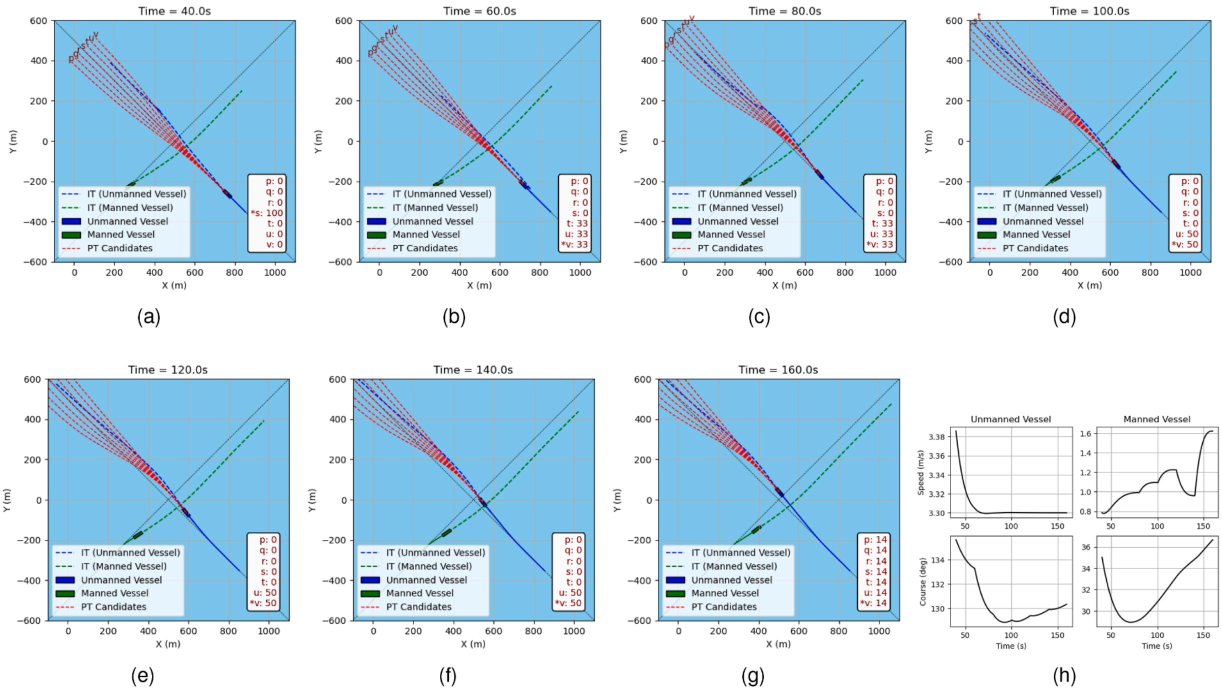

Fig. 5. Case Study 01: (a)–(g) Vessel positions during simulation. (h) Course and speed changes of the vessels over during the simulations.

Table 5
Evaluation results of the candidate trajectories at $t = 40s$ in Case Study 01.

Trajectory	C	SD_1	P_1	PA_1	SA_1	GS_1	C_OTing_1	C_HO_1	$C\_CR\_SS_1$	$C\_CR\_PS_1$
p	false	true	false	true	false	false	true	true	true	false
q	false	true	false	true	false	false	true	true	true	false
r	false	true	false	true	false	false	true	true	true	false
s*	true	true	false	false	false	true	true	true	true	true
t	false	true	false	false	true	true	true	true	true	true
u	false	true	false	false	true	true	true	true	true	true
v	false	true	false	false	true	true	true	true	true	true

Trajectory	C_OTen_1	CEM_1	SOC_1	GWC_1	R_1	$C\_COLAV\_M_1$	SDG_S	SDG	C_1
p	true	false	false	false	SO	false	true	true	false
q	true	false	false	false	SO	false	true	true	false
r	true	false	false	false	SO	false	true	true	false
s*	true	true	true	true	SO	true	true	true	true
t	true	true	false	true	SO	false	true	true	false
u	true	true	false	true	SO	false	true	true	false
v	true	true	false	true	SO	false	true	true	false

Table 6
Evaluation results of the candidate trajectories at $t = 60s$ in Case Study 01.

Trajectory	C	SD_1	P_1	PA_1	SA_1	GS_1	C_OTing_1	C_HO_1	$C\_CR\_SS_1$	$C\_CR\_PS_1$
p	false	true	false	true	true	false	true	true	true	false
q	false	true	false	true	true	false	true	true	true	false
r	false	true	false	true	true	false	true	true	true	false
s	false	true	false	true	true	false	true	true	true	false
t	true	true	false	false	true	true	true	true	true	true
u	true	true	false	false	true	true	true	true	true	true
v*	true	true	false	false	true	true	true	true	true	true

Trajectory	C_OTen_1	CEM_1	SOC_1	GWC_1	R_1	$C\_COLAV\_M_1$	SDG_S	SDG	C_1
p	true	false	false	false	GW	false	true	true	false
q	true	false	false	false	GW	false	true	true	false
r	true	false	false	false	GW	false	true	true	false
s	true	false	false	false	GW	false	true	true	false
t	true	true	false	true	GW	true	true	true	true
u	true	true	false	true	GW	true	true	true	true
v*	true	true	false	true	GW	true	true	true	true

Table 7
Evaluation results of the candidate trajectories at $t = 100s$ in Case Study 01.

Trajectory	C	SD_1	P_1	PA_1	SA_1	GS_1	C_OTing_1	C_HO_1	$C\_CR\_SS_1$	$C\_CR\_PS_1$
p	false	true	false	true	true	false	true	true	true	false
q	false	true	false	true	true	false	true	true	true	false
r	false	true	false	true	true	false	true	true	true	false
s	false	true	false	true	true	false	true	true	true	false
t	false	true	false	true	true	false	true	true	true	false
u	true	true	false	false	true	true	true	true	true	true
v*	true	true	false	false	true	true	true	true	true	true

Trajectory	C_OTen_1	CEM_1	SOC_1	GWC_1	R_1	$C\_COLAV\_M_1$	SDG_S	SDG	C_1
p	true	false	false	false	GW	false	true	true	false
q	true	false	false	false	GW	false	true	true	false
r	true	false	false	false	GW	false	true	true	false
s	true	false	false	false	GW	false	true	true	false
t	true	false	false	false	GW	false	true	true	false
u	true	true	false	true	GW	true	true	true	true
v*	true	true	false	true	GW	true	true	true	true

Table 8
Evaluation results of the candidate trajectories at $t = 160s$ in Case Study 01.

Trajectory	C	SD_1	P_1	PA_1	SA_1	GS_1	C_OTing_1	C_HO_1	$C\_CR\_SS_1$	$C\_CR\_PS_1$
p	true	true	true	true	true	false	true	true	true	false
q	true	true	true	true	true	false	true	true	true	false
r	true	true	true	true	true	false	true	true	true	false
s	true	true	true	true	true	false	true	true	true	false
t	true	true	true	true	true	false	true	true	true	false
u	true	true	true	false	true	true	true	true	true	true
v*	true	true	true	false	true	true	true	true	true	true

Trajectory	C_OTen_1	CEM_1	SOC_1	GWC_1	R_1	$C\_COLAV\_M_1$	SDG_S	SDG	C_1
p	true	false	false	false	GW	true	true	true	true
q	true	false	false	false	GW	true	true	true	true
r	true	false	false	false	GW	true	true	true	true
s	true	false	false	false	GW	true	true	true	true
t	true	false	false	false	GW	true	true	true	true
u	true	true	false	true	GW	true	true	true	true
v*	true	true	false	true	GW	true	true	true	true

manned vessel. Therefore, only those two candidates are considered to comply with the predicted intentions ($C = true$).

Again, from $t = 100s$ to $t = 140s$ the conditions remain the same. At $t = 160s$, the states of the modal variables in the DBN for each candidate trajectory are shown in Table 8.

In this iteration, all candidate trajectories pass the manned vessel safely ($P_1 = true$). Hence, all candidates are considered to be correct collision avoidance maneuvers ($C\_COLAV\_M_1 = true$). Thus, each candidate is intention compliant ($C = true$) and as a result equal probability is received by all.

4.2. Case study 02

In this case study (see Fig. 6), we observe a head-on collision scenario in which the manned vessel is cooperative. IT turns to starboard to avoid collision and expect the unmanned vessel to turn to starboard as well.

According to the DBN, it can be expected that the intentions of the unmanned vessel could be observed as shown in Table 9 at $t = 40, 60, 140s$ instances.

The states of the modal variables in the DBN for each candidate trajectory at $t = 40s$ are shown in Table 10.

The DBN predicts that the unmanned vessel intends to comply with COLREGS ($I_{CC} = true$) and intends to demonstrate good seamanship ($I_{GS} = true$). Since the intended COLREGS situation is determined head-on ($I_{CS_1} = HO$), following the definition of correct evasive maneuver ($CEM_i[t]$), only the trajectories that demonstrate correct head-on maneuvers ($C\_HO_1 = true$) are deemed correct evasive maneuvers, that is, u and v. Then these trajectories, in turn, also satisfy the give-way correct requirement ($GWC_1 = true$). Since the role is determined to be give-way ($R_1 = GW$), only these maneuvers are deemed to be correct collision avoidance maneuvers ($C\_COLAV\_M_1 = true$). As the unmanned vessel is considered to not intend to display unmodeled behavior ($I_U = false$), the candidates u and v are predicted to comply with intentions ($C = true$).

At $t = 60s$, the states of the modal variables in the DBN for each candidate trajectory are shown in Table 11.

The unmanned vessel is predicted to comply with COLREGS ($I_{CC} = true$) and the COLREGS situation is expected to be head-on ($I_{CS_1} = HO$). The candidate s, t, u, v trajectories evaluated as correct head-on

Table 9
The likely intentions of the unmanned vessel, as perceived from the perspective of the manned vessel at $t = 40, 60, 140$s in Case Study 02.

Node ID	State		
	$t = 40$	$t = 60$	$t = 140$
I_{SD}	State3	State3	State3
I_{SDF}	State3	State3	State3
I_{AT}	State4	State4	State4
I_{CC}	true	true	true
I_{CS_1}	HO	HO	HO
I_{GS}	true	true	true
I_{P_1}	similar	similar	similar
I_{SDM}	State4	State4	State4
I_U	false	false	false
I_G	false	false	false
I_{SDGS}	State3	State3	State3

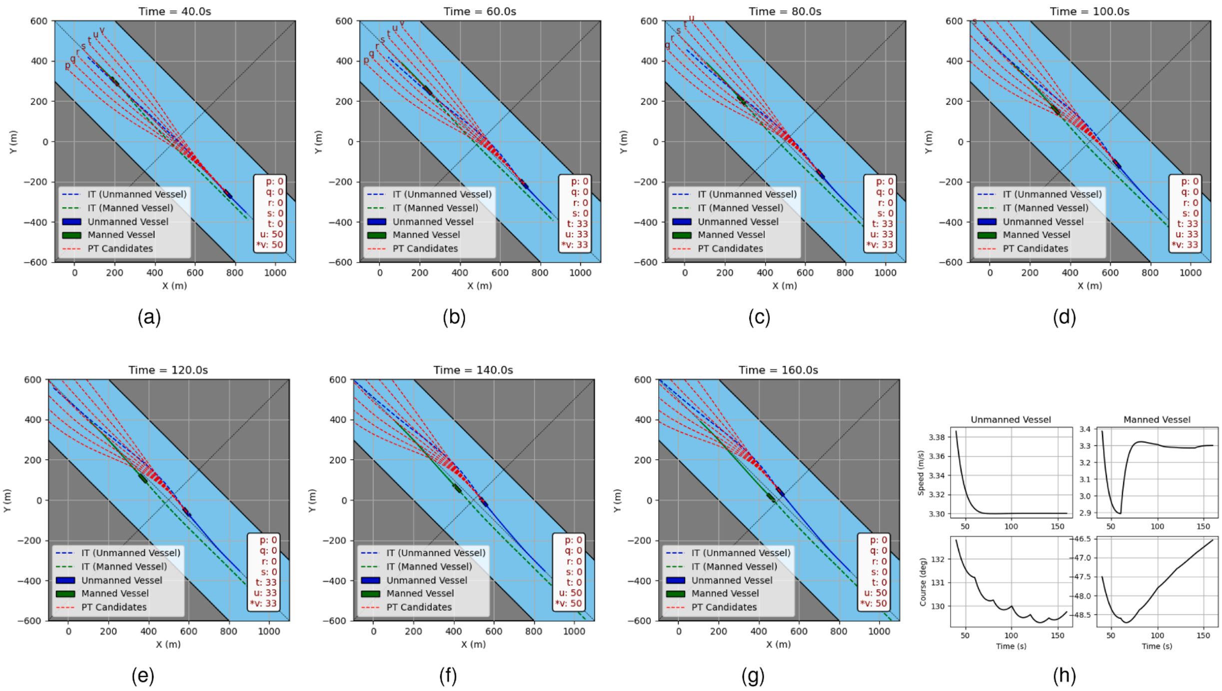

Fig. 6. Case Study 02: (a)–(g) Vessel positions during simulation. (h) Course and speed changes of the vessels over during the simulations.

Table 10
Evaluation results of the candidate trajectories at $t = 40s$ in Case Study 02.

Trajectory	C	SD_1	P_1	PA_1	SA_1	GS_1	C_OTing_1	C_HO_1	$C\_CR\_SS_1$	$C\_CR\_PS_1$
p	false	true	false	true	true	false	true	false	false	false
q	false	false	false	true	true	false	false	false	false	false
r	false	false	false	true	true	false	false	false	false	false
s	false	true	false	true	true	false	true	false	true	false
t	false	true	false	false	true	true	true	false	true	true
u	true	true	false	false	true	true	true	true	true	true
v*	true	true	false	false	true	true	true	true	true	true

Trajectory	C_OTen_1	CEM_1	SOC_1	GWC_1	R_1	$C\_COLAV\_M_1$	SDG_S	SDG	C_1
p	true	false	false	false	GW	false	true	true	false
q	false	false	false	false	GW	false	true	true	false
r	false	false	false	false	GW	false	true	true	false
s	true	false	false	false	GW	false	true	true	false
t	true	false	false	false	GW	false	true	true	false
u	true	true	false	true	GW	true	true	true	true
v*	true	true	false	true	GW	true	true	true	true

Table 11
Evaluation results of the candidate trajectories at $t = 60s$ in Case Study 02.

Trajectory	C	SD_1	P_1	PA_1	SA_1	GS_1	C_OTing_1	C_HO_1	$C\_CR\_SS_1$	$C\_CR\_PS_1$
p	false	true	false	true	true	false	true	false	true	false
q	false	true	false	true	true	false	true	false	true	false
r	false	true	false	true	true	false	true	false	true	false
s	false	true	false	true	true	false	true	true	true	false
t	true	true	false	false	true	true	true	true	true	true
u	true	true	false	false	true	true	true	true	true	true
v*	true	true	false	false	true	true	true	true	true	true

Trajectory	C_OTen_1	CEM_1	SOC_1	GWC_1	R_1	$C\_COLAV\_M_1$	SDG_S	SDG	C_1
p	true	false	false	false	GW	false	true	true	false
q	true	false	false	false	GW	false	true	true	false
r	true	false	false	false	GW	false	true	true	false
s	true	false	false	false	GW	false	true	true	false
t	true	true	false	true	GW	true	true	true	true
u	true	true	false	true	GW	true	true	true	true
v*	true	true	false	true	GW	true	true	true	true

Table 12
Evaluation results of the candidate trajectories at $t = 140s$ in Case Study 02.

Trajectory	C	SD_1	P_1	PA_1	SA_1	GS_1	C_OTing_1	C_HO_1	$C\_CR\_SS_1$	$C\_CR\_PS_1$
p	false	true	false	true	true	false	true	true	true	false
q	false	true	false	true	true	false	true	true	true	false
r	false	true	false	true	true	false	true	true	true	false
s	false	true	false	true	true	false	true	true	true	false
t	false	true	false	true	true	false	true	true	true	false
u	true	true	false	false	true	true	true	true	true	true
v*	true	true	false	false	true	true	true	true	true	true

Trajectory	C_OTen_1	CEM_1	SOC_1	GWC_1	R_1	$C\_COLAV\_M_1$	SDG_S	SDG	C_1
p	true	false	false	false	GW	false	true	true	false
q	true	false	false	false	GW	false	true	true	false
r	true	false	false	false	GW	false	true	true	false
s	true	false	false	false	GW	false	true	true	false
t	true	false	false	false	GW	false	true	true	false
u	true	true	false	true	GW	true	true	true	true
v*	true	true	false	true	GW	true	true	true	true

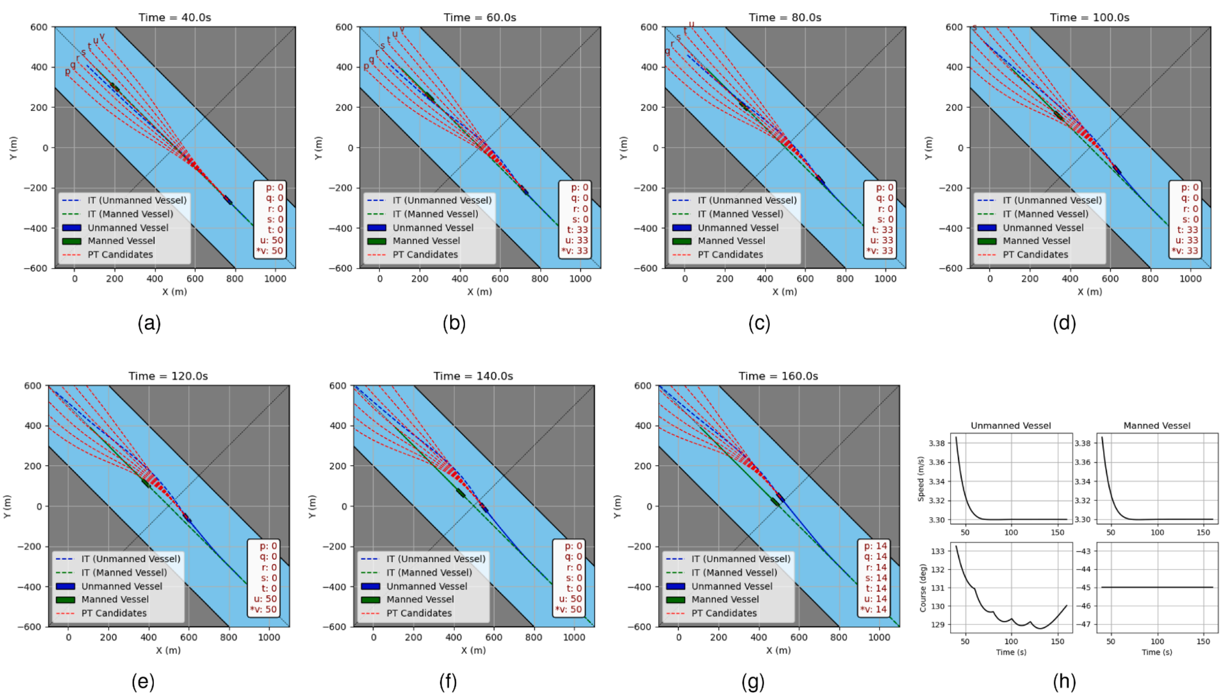

Fig. 7. Case Study 03: (a)–(g) Vessel positions during simulation. (h) Course and speed changes of the vessels over during the simulations.

Table 13
The likely intentions of the unmanned vessel, as perceived from the perspective of the manned vessel at $t = 40, 60, 120, 160s$ in Case Study 03.

Node ID	State			
	t = 40	t = 60	t = 120	t = 160
I_{SD}	State3	State3	State3	State3
I_{SDF}	State3	State3	State3	State3
I_{AT}	State4	State4	State4	State4
I_{CC}	true	true	true	true
I_{CS_1}	HO	HO	HO	HO
I_{GS}	true	true	true	true
I_{P_1}	similar	similar	similar	similar
I_{SDM}	State4	State4	State4	State4
I_U	false	false	false	false
I_G	false	false	false	false
I_{SDGS}	State3	State3	State3	State3

maneuvers ($C\_HO_1 = true$). However, only t, u, v display good seamanship ($GS_1 = true$). Therefore, only t, u, v trajectories are evaluated to show correct evasive maneuvers ($CEM_1 = true$). As a result, it can be seen that the same trajectories are evaluated to be complaint with the predicted intentions ($C = true$).

From $t = 60s$ to $t = 120s$ the conditions remain the same. At $t = 140s$, the states of the modal variables in the DBN for each candidate trajectory are shown in Table 12.

The predicted intentions do not change since $t = 60s$. Instead, all candidate trajectories become eligible to be considered correct head-on maneuvers (C_{HO_1}). However, only u and v promote good seamanship ($GS_1 = true$) at this time. Hence, they are evaluated as the only candidates that comply with the intentions ($C = true$). This is maintained from $t = 140s$ through $t = 160s$ until the candidate trajectories pass the manned vessel safely ($P_1 = true$).

4.3. Case study 03

In this case study (see Fig. 7), we observe another head-on collision scenario. However, in this case, the manned vessel is non-cooperative in the sense that it does not make a starboard turn and instead keeps

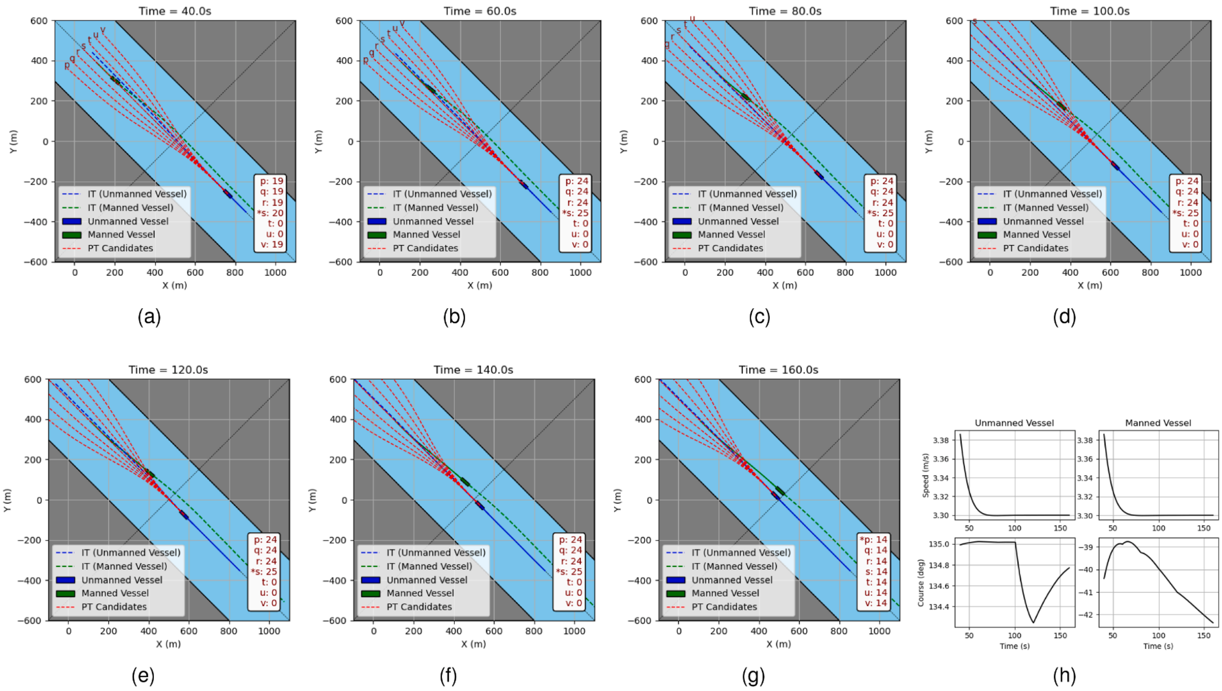

Fig. 8. Case Study 04: (a)–(g) Vessel positions during simulation. (h) Course and speed changes of the vessels over during the simulations.

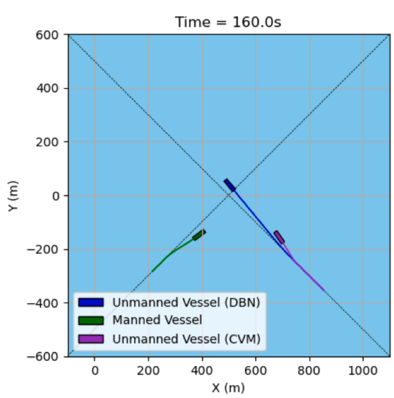

Fig. 9. Side-by-side comparison of trajectories when using DBN and CVM for predicting PT of the manned vessel at $t = 160s$ in Case study 01.

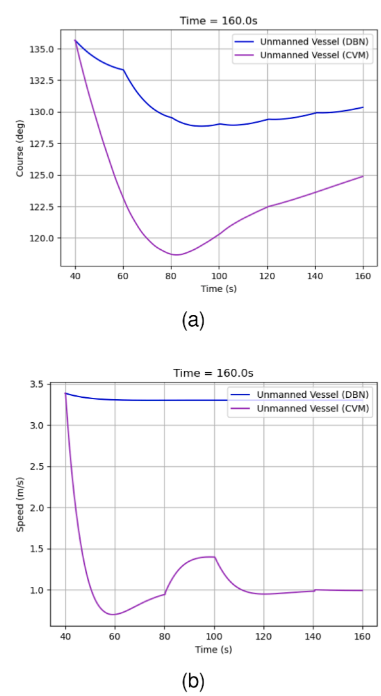

Fig. 10. Side-by-side comparison of course and speed change when using DBN and CVM for predicting PT of the manned vessel at $t = 160s$ in Case study 01.

the same course and speed. The manned vessel requires the unmanned vessel to make a larger course change to avoid collision.

According to the DBN, it can be expected that the intentions of the unmanned vessel could be observed as shown in Table 13 at $t = 40, 60, 120, 160s$ instances.

The states of the modal variables in the DBN for each candidate trajectory at $t = 40s$ are shown in Table 14.

The DBN predicts that the unmanned vessel intends to comply with COLREGS ($I_{CC} = true$) and that the intended situation of COLREGS is head-on ($I_{CS_1} = HO$). It also predicts that it intends to demonstrate good seamanship ($I_{GS} = true$). Therefore, following the definition of the correct evasive maneuver ($CEM_i[t]$), only the trajectories u and v are predicted to be compliant with the requirements as they are both correct head-on maneuvers ($C\_HO_1 = true$), and complete good seamanship conditions ($GS_1 = true$). Since the role of the unmanned vessel is predicted to be give-way ($R_1 = GW$), the candidates that display correct collision avoidance maneuvers ($C\_COLAV\_M_1 = true$) are the correct give-way maneuvers ($GWC_1 = true$). The candidates u and v satisfy this requirement by being correct evasive maneuvers ($CEM_1 = true$). As the unmanned vessel is considered to not intend to display unmodeled behavior ($I_U = false$), the candidates u and v are predicted to comply with intentions ($C = true$).

At $t = 60s$, the states of the modal variables in the DBN for each candidate trajectory are shown in Table 15.

In this iteration, the intentions remain the same as when $t = 40s$. However, more candidate trajectories (s, t, u, v) have now become eligible to be correct head-on maneuvers ($C\_HO_1 = true$). Of these, candi-

Table 14
Evaluation results of the candidate trajectories at $t = 40s$ in Case Study 03.

Trajectory	C	SD_1	P_1	PA_1	SA_1	GS_1	C_OTing_1	C_HO_1	$C\_CR\_SS_1$	$C\_CR\_PS_1$
p	false	true	false	true	true	false	true	false	false	false
q	false	true	false	true	true	false	true	false	false	false
r	false	false	false	true	true	false	false	false	false	false
s	false	false	false	true	true	false	false	false	false	false
t	false	false	false	false	true	true	false	false	false	false
u	true	true	false	false	true	true	true	true	true	true
v*	true	true	false	false	true	true	true	true	true	true

Trajectory	C_OTen_1	CEM_1	SOC_1	GWC_1	R_1	$C\_COLAV\_M_1$	SDG_S	SDG	C_1
p	true	false	false	false	GW	false	true	true	false
q	true	false	false	false	GW	false	true	true	false
r	false	false	false	false	GW	false	true	true	false
s	false	false	false	false	GW	false	true	true	false
t	false	false	false	false	GW	false	true	true	false
u	true	true	false	true	GW	true	true	true	true
v*	true	true	false	true	GW	true	true	true	true

Table 15
Evaluation results of the candidate trajectories at $t = 60s$ in Case Study 03.

Trajectory	C	SD_1	P_1	PA_1	SA_1	GS_1	C_OTing_1	C_HO_1	$C\_CR\_SS_1$	$C\_CR\_PS_1$
p	false	true	false	true	true	false	true	false	false	false
q	false	true	false	true	true	false	true	false	false	false
r	false	true	false	true	true	false	true	false	true	false
s	false	true	false	true	true	false	true	true	true	false
t	true	true	false	false	true	true	true	true	true	true
u	true	true	false	false	true	true	true	true	true	true
v*	true	true	false	false	true	true	true	true	true	true

Trajectory	C_OTen_1	CEM_1	SOC_1	GWC_1	R_1	$C\_COLAV\_M_1$	SDG_S	SDG	C_1
p	true	false	false	false	GW	false	true	true	false
q	true	false	false	false	GW	false	true	true	false
r	true	false	false	false	GW	false	true	true	false
s	true	false	false	false	GW	false	true	true	false
t	true	true	false	true	GW	true	true	true	true
u	true	true	false	true	GW	true	true	true	true
v*	true	true	false	true	GW	true	true	true	true

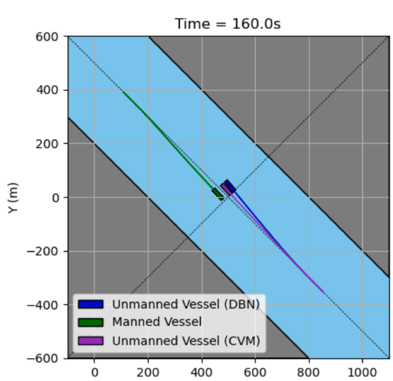

Fig. 11. Side-by-side comparison of trajectories when using DBN and CVM for predicting PT of the manned vessel at $t = 160s$ in Case study 02.

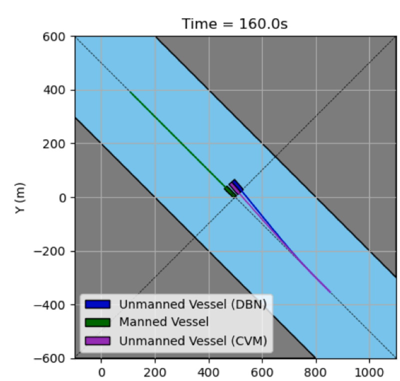

Fig. 12. Side-by-side comparison of trajectories when using DBN and CVM for predicting PT of the manned vessel at $t = 160s$ in Case study 03.

dates t, u, v maintain good seamanship maneuvers ($GS_1 = true$) and are therefore evaluated as compliant with intentions (C).

From $t = 60s$ to $t = 100s$ the conditions remain the same. At $t = 120s$, the states of the modal variables in the DBN for each candidate trajectory are shown in Table 16.

The predicted intentions do not change. Instead, all candidate trajectories become eligible to be considered correct head-on maneuvers (C_{HO_1}). However, only u and v promote good seamanship ($GS_1 = true$) at this time. Hence, they are evaluated as the only candidates that comply with the intentions ($C = true$).

The conditions remain the same for the $t = 120s$ and $t = 140s$ time steps. At $t = 160s$, the states of the modal variables in the DBN for each candidate trajectory are shown in Table 17.

Since all candidate trajectories pass the manned vessel safely ($P_1 = true$), each and every candidate is intention-compliant (C) and as a result equal probability is received by all.

Table 16
Evaluation results of the candidate trajectories at $t = 120s$ in Case Study 03.

Trajectory	C	SD_1	P_1	PA_1	SA_1	GS_1	C_OTing_1	C_HO_1	$C\_CR\_SS_1$	$C\_CR\_PS_1$
p	false	true	false	true	true	false	true	true	true	false
q	false	true	false	true	true	false	true	true	true	false
r	false	true	false	true	true	false	true	true	true	false
s	false	true	false	true	true	false	true	true	true	false
t	false	true	false	true	true	false	true	true	true	false
u	true	true	false	false	true	true	true	true	true	true
v*	true	true	false	false	true	true	true	true	true	true

Trajectory	C_OTen_1	CEM_1	SOC_1	GWC_1	R_1	$C\_COLAV\_M_1$	SDG_S	SDG	C_1
p	true	false	false	false	GW	false	true	true	false
q	true	false	false	false	GW	false	true	true	false
r	true	false	false	false	GW	false	true	true	false
s	true	false	false	false	GW	false	true	true	false
t	true	false	false	false	GW	false	true	true	false
u	true	true	false	true	GW	true	true	true	true
v*	true	true	false	true	GW	true	true	true	true

Table 17
Evaluation results of the candidate trajectories at $t = 160s$ in Case Study 03.

Trajectory	C	SD_1	P_1	PA_1	SA_1	GS_1	C_OTing_1	C_HO_1	$C\_CR\_SS_1$	$C\_CR\_PS_1$
p	true	true	true	true	true	false	true	true	true	false
q	true	true	true	true	true	false	true	true	true	false
r	true	true	true	true	true	false	true	true	true	false
s	true	true	true	true	true	false	true	true	true	false
t	true	true	true	true	true	false	true	true	true	false
u	true	true	true	false	true	true	true	true	true	true
v*	true	true	true	false	true	true	true	true	true	true

Trajectory	C_OTen_1	CEM_1	SOC_1	GWC_1	R_1	$C\_COLAV\_M_1$	SDG_S	SDG	C_1
p	true	false	false	false	GW	true	true	true	true
q	true	false	false	false	GW	true	true	true	true
r	true	false	false	false	GW	true	true	true	true
s	true	false	false	false	GW	true	true	true	true
t	true	false	false	false	GW	true	true	true	true
u	true	true	false	true	GW	true	true	true	true
v*	true	true	false	true	GW	true	true	true	true

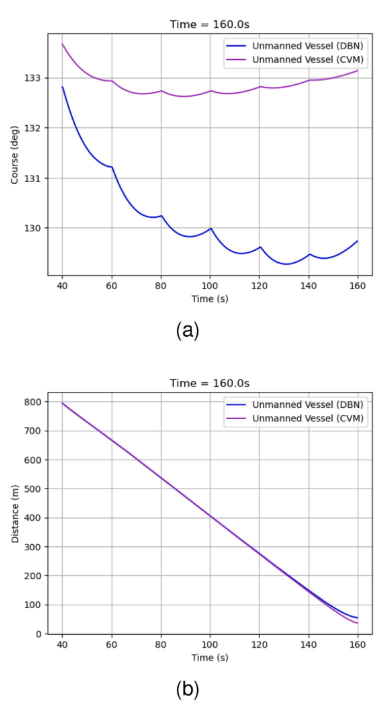

Fig. 13. Side-by-side comparison of course and distance change when using DBN and CVM for predicting PT of the manned vessel at $t = 160s$ in Case study 02.

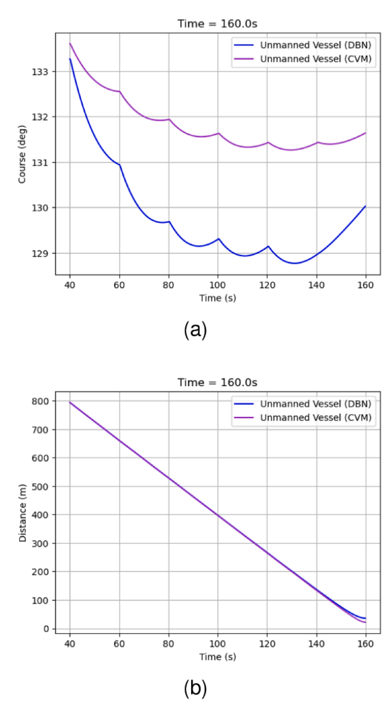

Fig. 14. Side-by-side comparison of course and distance change when using DBN and CVM for predicting PT of the manned vessel at $t = 160s$ in Case study 03.

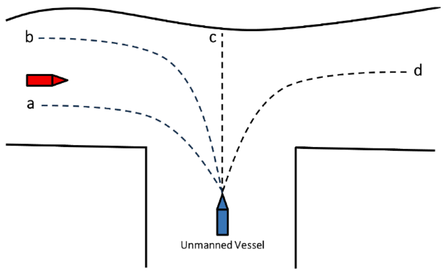

Fig. 15. Example test case that includes grounding hazards in close proximity of the vessels.

Table 18
The likely intentions of the unmanned vessel, as perceived from the perspective of the manned vessel at $t = 40, 60, 160s$ in Case Study 04.

Node ID	State		
	t = 40	t = 60	t = 160
I_{SD}	State3	State3	State3
I_{SDF}	State3	State3	State3
I_{AT}	State4	State4	State4
I_{CC}	false	false	false
I_{CS_1}	HO	HO	HO
I_{GS}	true	true	true
I_{P_1}	similar	similar	similar
I_{SDM}	State4	State4	State4
I_U	false	false	false
I_G	false	false	false
I_{SDGS}	State3	State3	State3

4.4. Case study 04

The last case study is a scenario in which the manned vessel clearly violates the COLREGS by steering to the port side in a head-on scenario (see Fig. 8). In this situation, the PT of the manned vessel could be interpreted as wanting the unmanned vessel to cooperate by steering to the port side. The purpose of this case study is to verify that the PT prediction can accurately predict a person's PT, even in cases where this PT is against traffic regulations.

According to the DBN, it can be expected that the intentions of the unmanned vessel could be observed as shown in Table 18 at $t = 40, 60, 160s$ instances.

At $t = 40s$, the states of the modal variables in the DBN for each candidate trajectory are shown in Table 19.

Since the manned vessel intends to not comply with COLREGS, the DBN predicts that the unmanned vessel could also intend to do the same as indicated by $I_{CC} = false$. According to the definition of correct evasive maneuver ($CEM_i[t]$), candidate trajectories that comply with intentions must be in a correct head-on maneuver ($C\_HO_1 = true$) or have a safe distance at CPA ($SD_1 = true$) when $I_{CC} = false$. The u and v trajectories meet the first requirement, while the p, q, r, s, t fulfill the latter. In either case, the candidate must also comply with the good seamanship requirement stated in $CEM_i[t]$ definition. Since DBN predicts that the unmanned vessel intends to maintain good seamanship ($I_{GS} = true$), only candidates that meet the $GS_1 = true$ condition are eligible. Therefore, only candidates p, q, r, s, v comply with the intentions predicted, as indicated by $C = true$.

At $t = 60s$, the states of the modal variables in the DBN for each candidate trajectory are shown in Table 20.

The DBN deems that the unmanned vessel continues to be not COLREGS compliant ($I_{CC} = false$). Hence, similar conditions as when $t = 40s$ apply when determining whether each candidate trajectory is considered as a correct evasive maneuver ($CEM_1 = true$). Since $C\_HO_1 = true$ for candidates t, u, v, and $SD_1 = true$ for all candidates, again GS_1 becomes the deciding factor. Only candidates p, q, r, s are marked with $GS_1 = true$. Thus, only those are considered compatible with the intentions predicted ($C = true$).

From $t = 60s$ to $t = 140s$ the conditions remain the same. At $t = 160s$, the states of the modal variables in the DBN for each candidate trajectory are shown in Table 21.

In this iteration, all candidate trajectories pass the manned vessel safely ($P_1 = true$). Hence, all candidates are considered to be correct collision avoidance maneuvers ($C\_COLAV\_M_1 = true$). Thus, each candidate is intention compliant ($C = true$) and as a result equal probability is received by all.

4.5. Comparisons

To determined the effectiveness of the DBN in predicting manned PT, a comparison was drawn between that and assuming a straight-line trajectory. To facilitate this comparison, the PT prediction component of HM-CCAS using the DBN was replaced by a CVM that would extrapolate the current state of the unmanned vessel to create a trajectory. This trajectory is then used as the PT of the manned vessel. The straight-line trajectory is selected as a baseline because it is the simplest and most straightforward form of trajectory that can be expected from a manned vessel.

In **Case study 01**, first the trajectories were observed side-by-side and the result is depicted in Fig. 9. It could be observed that the trajectory with DBN for the prediction completes the collision avoidance maneuver much faster than that with CVM for the prediction. At $t = 160s$, the one with DBN has already completed its collision avoidance maneuver. Since the manned vessel follows a pre-defined path, one with the CVM even risks running into a collision. However, in a real situation, the manned vessel is bound to make the necessary adjustments to its course or speed to avoid collision.

The **Case study 01** demonstrates a crossing scenario. According to COLREGS Rule 15 which governs similar situations, the vessel which has the other vessel on its starboard side needs to give way. In this case, the manned vessel must give-way while the unmanned vessel stand-on. According to COLREGS Rule 17 (a–i), the stand-on vessel shall keep her course and speed constant so that the give-way vessel can plan its collision avoidance trajectory without uncertainty. However, according to Rule 17 (a–ii), the stand-on vessel is allowed to take action and perform a starboard maneuver when it finds itself so close that the collision cannot be avoided by the action of the give-way vessel alone.

When observing the course and speed change between the two prediction methods, it was observed that the one with the CVM performs a much larger course change and a speed change (see Fig. 10). In CCAS-Proto, PT is essentially what the vessel wants the other vessel to follow. Hence, the HM-CCAS algorithm tries to accommodate this as much as possible when generating a safe passage, that is, IT. When PT of the manned vessel is generated using a CVM, it is essentially asking the unmanned vessel to stand-on in the current heading direction since CVM just extrapolates the current state of the ship. Therefore, a course change tends not to show up inside the decision loop in the first few iterations. As the heading direction in the first few iterations is on a collision course, the algorithm resorts to reducing the speed to avoid collision. These iterations at the beginning are propagated to the future time steps as well due to the nature of the algorithm, resulting in a significant speed reduction and a larger course change. On the other hand, there is almost no change in speed and a minimal change in course from the one with the DBN. In our opinion, this is a better reaction as it does the bare minimum to avoid collision without creating uncertainty about its decision from the point of view of the manned vessel.

Case study 02 and **Case study 03** demonstrate a head-on scenario in which the manned vessel is cooperative and non-cooperative respectively. The trajectories in this instance when using DBN and CVM are depicted in Figs. 11 and 12. According to COLREGS Rule 14 which gov-

Table 19
Evaluation results of the candidate trajectories at $t = 40s$ in Case Study 04.

Trajectory	C	SD_1	P_1	PA_1	SA_1	GS_1	C_OTing_1	C_HO_1	$C\_CR\_SS_1$	$C\_CR\_PS_1$
p	true	true	false	true	false	true	true	false	false	false
q	true	true	false	true	false	true	true	false	false	false
r	true	true	false	true	false	true	true	false	false	false
s*	true	true	false	false	false	true	true	false	false	true
t	false	true	false	false	true	false	true	false	false	true
u	false	false	false	false	true	false	false	true	false	false
v	true	false	false	false	true	true	false	true	false	false

Trajectory	C_OTen_1	CEM_1	SOC_1	GWC_1	R_1	$C\_COLAV\_M_1$	SDG_S	SDG	C_1
p	true	true	false	true	GW	true	true	true	true
q	true	true	false	true	GW	true	true	true	true
r	true	true	false	true	GW	true	true	true	true
s*	true	true	true	true	GW	true	true	true	true
t	true	false	false	false	GW	false	true	true	false
u	false	false	false	false	GW	false	true	true	false
v	false	true	false	true	GW	true	true	true	true

Table 20
Evaluation results of the candidate trajectories at $t = 60s$ in Case Study 04.

Trajectory	C	SD_1	P_1	PA_1	SA_1	GS_1	C_OTing_1	C_HO_1	$C\_CR\_SS_1$	$C\_CR\_PS_1$
p	true	true	false	true	false	true	true	false	false	false
q	true	true	false	true	false	true	true	false	false	false
r	true	true	false	true	false	true	true	false	false	false
s*	true	true	false	false	false	true	true	false	false	true
t	false	true	false	false	true	false	true	true	false	true
u	false	true	false	false	true	false	true	true	false	true
v	false	true	false	false	true	false	true	true	false	true

Trajectory	C_OTen_1	CEM_1	SOC_1	GWC_1	R_1	$C\_COLAV\_M_1$	SDG_S	SDG	C_1
p	true	true	false	true	GW	true	true	true	true
q	true	true	false	true	GW	true	true	true	true
r	true	true	false	true	GW	true	true	true	true
s*	true	true	true	true	GW	true	true	true	true
t	true	false	false	false	GW	false	true	true	false
u	true	false	false	false	GW	false	true	true	false
v	true	false	false	false	GW	false	true	true	false

Table 21
Evaluation results of the candidate trajectories at $t = 160s$ in Case Study 04.

Trajectory	C	SD_1	P_1	PA_1	SA_1	GS_1	C_OTing_1	C_HO_1	$C\_CR\_SS_1$	$C\_CR\_PS_1$
p*	true	true	true	true	false	true	true	false	false	false
q	true	true	true	true	false	true	true	false	false	false
r	true	true	true	true	false	true	true	false	false	false
s	true	true	true	false	false	true	true	false	false	true
t	true	true	true	false	true	false	true	false	false	true
u	true	true	true	false	true	false	true	false	false	true
v	true	true	true	false	true	false	true	false	false	true

Trajectory	C_OTen_1	CEM_1	SOC_1	GWC_1	R_1	$C\_COLAV\_M_1$	SDG_S	SDG	C_1
p*	true	true	false	true	GW	true	true	true	true
q	true	true	false	true	GW	true	true	true	true
r	true	true	false	true	GW	true	true	true	true
s	true	true	true	true	GW	true	true	true	true
t	true	false	false	false	GW	true	true	true	true
u	true	false	false	false	GW	true	true	true	true
v	true	false	false	false	GW	true	true	true	true

erns such situations, both vessels are obliged to give-way by turning to their respective starboard side. However, if the manned vessel does not comply, the unmanned vessel is required to identify the situation early on and make a larger turn.

When observing the course change of the two instances, it was evident that the one with the DBN acts earlier with a significantly larger course change than the one with the CVM. In addition, when the Euclidean distance was calculated between the unmanned and manned vessels during the two instances, the one with the DBN had a greater safety margin in line with the earlier and more significant maneuver taken by it when using the DBN. These results are shown in Fig. 13 for **Case study 02** and Fig. 14 for **Case study 03**.

In **Case study 04** the DBN did not provide a significant advantage over using the CVM, since the former also produces a similar straight-line trajectory to avoid collision in that scenario. Therefore, in the interest of brevity, we decided not to include it here.

5. Discussion and conclusions

This paper presents a novel collaborative collision avoidance algorithm, HM-CCAS, that enables a vessel to collaborate with manned and unmanned vessels in the vicinity to obtain a safe passage. The groundwork leading to this result has been laid in Tran et al. (2025), where the authors propose a collaborative collision avoidance algorithm for situations where only unmanned vessels exist. The authors of Tran et al. (2025) propose a CCAS-Proto, which is a protocol defined to exchange data consisting of IT and PT. This method isn't viable for mixed traffic scenarios where both manned and unmanned vessels are present, since a manned vessel cannot be expected to have the computational capability to produce a PT. Hence, we propose a DBN that would enable an unmanned vessel to predict the PT of the manned vessel on its own based on the states of the vessels and IT of the manned vessel, thus enabling CCAS-Proto. This new algorithm was named HM-CCAS.

To evaluate the algorithm, a series of simulation studies were conducted considering various COLREGS scenarios. Due to space limitations only a selected number of cases which include compliant, partially compliant, and non-compliant COLREGS scenarios are presented in the paper. To validate the importance of predicting PT using a DBN, the case studies presented in this article were subjected to a comparison in which PT of manned vessel was calculated using a CVM instead of predicting via the DBN proposed in this article.

The results showed that HM-CCAS is a viable collaborative collision avoidance algorithm for safe navigation. Comparisons with the CVM highlighted the importance of the DBN, as it is able to capture the intentions of unmanned vessels related to the interpretation of COLREGS and compliance with the rules. An aspect that was not tried in the comparison is the behavior when grounding hazards are present in close proximity. Such scenarios could perhaps provide the strongest argument in favor of using the DBN. However, such cases were not included in this paper for multiple reasons. Observe the scenario depicted in Fig. 15. The unmanned vessel could follow any of the a, b, d trajectories. IT will depend on its intention to be COLREGS compliant, the next waypoint to which the unmanned vessel intends to sail, and its intentions regarding the avoidance of grounding hazards. The DBN proposed in Mahipala et al. (2025) could capture all these intentions. However, the DBN proposed in this paper is a simplified version of the one from Mahipala et al. (2025), since the objective of is to establish whether the DBN is a viable solution to complete the CCAS-Proto in HM-CCAS algorithm. The other reason is that the current cost function in the HM-CCAS which was initially proposed in Tran et al. (2025) does not consider grounding hazards. In addition, the method proposed for candidate trajectory generation in this paper could not generate arbitrary trajectories similar to a, b, d presented in Fig. 15. On the other hand, if a CVM is used, it will give an output similar to the trajectory c, which is highly unlikely.

For future work, we plan to enhance the HM-CCAS algorithm to address grounding hazards. In addition, we hope to conduct scaled experiments with human-in-the-loop scenarios to understand the performance of HM-CCAS under real-world conditions and observe the real-time performance of the algorithm.

CRediT authorship contribution statement

Dhanika Mahipala: Writing – review & editing, Writing – original draft, Visualization, Validation, Software, Methodology, Investigation, Formal analysis, Conceptualization; **Hoang Anh Tran:** Writing – review & editing, Writing – original draft, Visualization, Validation, Software, Methodology, Investigation, Formal analysis, Conceptualization; **Rana Saha:** Writing – original draft, Investigation, Conceptualization; **Tor Arne Johansen:** Writing – review & editing, Supervision, Resources, Project administration, Investigation, Funding acquisition, Conceptualization.

Declaration of competing interest

The authors declare that they have no known competing financial interests or personal relationships that could have appeared to influence the work reported in this paper.

Appendix A. Appendix

The DBN from Mahipala et al. (2025) has been modified for the purpose of this paper. The following paragraphs list the Conditional Probability Tables (CPTs) for each modified model node, expressed in the form of equations.

When intending to be not COLREGS compliant (I_{CC}), a safe distance (SD_i) must be maintained to be a correct evasive maneuver (CEM_i). Hence, following (Tengesdal et al., 2024), the definition of CEM_i was changed to,

$$\begin{aligned} CEM_i[t] = {} & (\neg I_{GS} \vee GS_i[t]) \wedge \\ & \Big((\neg I_{cc} \wedge SD_i[t]) \\ & \vee (I_{CS_i} == OT\_ing \wedge C\_OTing_i[t]) \\ & \vee (I_{CS_i} == OT\_en \wedge C\_OTen_i[t]) \\ & \vee (I_{CS_i} == HO \wedge C\_HO_i[t]) \\ & \vee (I_{CS_i} == CR\_SS \wedge C\_CR\_SS_i[t]) \\ & \vee (I_{CS_i} == CR\_PS \wedge C\_CR\_PS_i[t]) \Big) \end{aligned} \tag{A.1}$$

The safe distance to ground (SDG) has been modified to exclude grounding considerations at the front of the vessel for simplicity. Adding it back would not have an impact on the outcome.

$$SDG[t] = SDG\_S[t] \tag{A.2}$$

Since next waypoint information is not considered, the correct collision avoidance maneuver ($C\_COLAV\_M_i$) should also take into account the case where the *reference vessel* safely passes the *obstacle vessel* (P_i). Therefore, the definition was changed to,

$$\begin{aligned} C\_COLAV\_M_i[t] = {} & \big(\neg P_i[t] \wedge (R_i[t] == SO) \wedge SOC_i[t]\big) \\ & \vee \\ & \big(\neg P_i[t] \wedge (R_i[t] == GW) \wedge GWC_i[t]\big) \\ & \vee \\ & P_i[t] \end{aligned} \tag{A.3}$$

The compatibility of intentions and measurements with the ship i (C_i) was modified to remove the consideration of information on the next waypoint.

$$C_i[t] = C\_COLAV\_M_i[t] \wedge (SDG_i[t] \vee I_G) \tag{A.4}$$

An observation is compatible with the reference ship's intention if it is compatible with all ships in the area (C_i) or if the ship intends to act in an unmodeled manner (I_U).

$$C[t] = (\wedge_{i=1}^{n} C_i[t]) \vee I_U \tag{A.5}$$

References

Akdağ, M., Pedersen, T.A., Fossen, T.I., Johansen, T.A., 2024a. A decision support system for autonomous ship trajectory planning. Ocean Eng. 292, 116562.

Akdağ, M., Tran, H.A., Lauvås, N., Pedersen, T.A., Fossen, T.I., Johansen, T.A., 2024b. A decentralized negotiation protocol for collaborative collision avoidance of autonomous surface vehicles. Authorea Prepr. 34 (2), 1016–1022. https://doi.org/10.1109/TCST.2025.3619554

Akdağ, M., Solnør, P., Johansen, T.A., 2022. Collaborative collision avoidance for maritime autonomous surface ships: a review. Ocean Eng. 250, 110920. https://doi.org/10.1016/j.oceaneng.2022.110920

BayesFusion, L., 2021a. GeNIe modeler. http://www.bayesfusion.com/.

BayesFusion, L., 2021b. Smile engine. http://www.bayesfusion.com/.

Chen, L., Hopman, H., Negenborn, R.R., 2018. Distributed model predictive control for vessel train formations of cooperative multi-vessel systems. Transp. Res. Part C Emerging Technol. 92, 101–118.

Dagum, P., Galper, A., Horvitz, E., 1992. Dynamic network models for forecasting. In: Proceedings of the Eighth International Conference on Uncertainty in Artificial Intelligence. Morgan Kaufmann Publishers Inc., San Francisco, CA, USA, pp. 41–48.

Ferranti, L., Negenborn, R.R., Keviczky, T., Alonso-Mora, J., 2018. Coordination of multiple vessels via distributed nonlinear model predictive control. In: 2018 European Control Conference (ECC). IEEE, Limassol, Cyprus, pp. 2523–2528.

International Hydrographic Organization, 2025. Major milestone achieved in transition to smart navigation with operational editions of s-100 standards. Accessed: 2025-04-09. https://iho.int/en/major-milestone-achieved-in-transition-to-smart-navigation-with-operational-editions-of-s-100-standards.

International Hydrographic Organization (IHO), 2020. S-100 framework: product specifications. https://iho.int/en/s-100-based-product-specifications. Retrieved from the International Hydrographic Organization website.

International Maritime Organization (IMO), 1972. Convention on the International Regulations for Preventing Collisions at Sea (COLREGs). International Maritime Organization.

International Maritime Organization (IMO), 2015. AIS Guidelines and Performance Standards (MSC.74(69)). IMO Publications.

International Association of Marine Aids to Navigation and Lighthouse Authorities (IALA), 2016. AIS Application Guidelines. IALA Standards.

International Maritime Organization (IMO), 2018. Imo takes first steps to address autonomous ships. Accessed: 2025-04-07. https://www.imo.org/en/MediaCentre/PressBriefings/Pages/08-MSC-99-MASS-scoping.aspx.

Koller, D., Friedman, N., 2009. Probabilistic Graphical Models: Principles and Techniques. The MIT Press, Cambridge, MA. 1st edition edition.

Mahipala, D., Tengesdal, T., Rokseth, B., Johansen, T.A., 2025. Design and validation of an intention-aware probabilistic framework for trajectory prediction: Integrating COLREGS, grounding hazards, and planned routes. Ocean Eng. 335, 121564. https://linkinghub.elsevier.com/retrieve/pii/S0029801825012703. https://doi.org/10.1016/j.oceaneng.2025.121564

Rothmund, S.V., Haugen, H.E., Veglo, G.D., Brekke, E.F., Johansen, T.A., 2023. Validation of ship intention model for maritime collision avoidance control using historical AIS data. In: 2023 European Control Conference (ECC), pp. 1–8. https://doi.org/10.23919/ECC57647.2023.10178133

Rothmund, S.V., Tengesdal, T., Brekke, E.F., Johansen, T.A., 2022. Intention modeling and inference for autonomous collision avoidance at sea. Ocean Eng. 266, 113080. https://doi.org/10.1016/j.oceaneng.2022.113080

Saha, R., Lundh, M., MacKinnon, S.N., 2023. The shift toward autonomous european inland waterway shipping: Identifying the gaps in the emerging socio-technical system. In: Journal of Physics: Conference Series. Vol. 2618. IOP Publishing, p. 012016.

Tengesdal, T., Rothmund, S., Basso, E., Schmidt-Didlaukies, H., Johansen, T., 2024. Obstacle intention awareness in automatic ship collision avoidance: full-scale experiments in confined waters. Field Rob. 4 (1), 211–245. https://doi.org/10.55417/fr.2024007

Tran, H.A., Johansen, T.A., Negenborn, R.R., 2024. Distributed MPC for autonomous ships on inland waterways with collaborative collision avoidance. http://arxiv.org/abs/2403.00554.

Tran, H.A., Lauvås, N., Johansen, T.A., Negenborn, R.R., 2025. Asynchronous Distributed Collision Avoidance With Intention Consensus for Inland Autonomous Ships. IEEE Trans. Control Syst. Technol. 33 (6) 1–16.